International Journal for Parasitology 41 (2011) 89–98

Contents lists available at ScienceDirect

International Journal for Parasitology

journal homepage: www.elsevier.com/locate/ijpara

Population genetic structure and history of a generalist parasite infecting multiple sympatric host species ☆

Elizabeth A. Archie [a,b,*], Vanessa O. Ezenwa [a,c]

[a] Division of Biological Sciences, University of Montana, Missoula, MT, USA
[b] Department of Biological Sciences, University of Notre Dame, Notre Dame, IN, USA
[c] Odum School of Ecology & Department of Infectious Diseases, University of Georgia Athens, GA, USA

ARTICLE INFO

Article history:
Received 7 April 2010
Received in revised form 17 July 2010
Accepted 26 July 2010

Keywords:
Helminths
Population genetic structure
Generalist
Ungulates
Gene flow
Host specificity
Evolutionary potential
Trichostrongylus axei

ABSTRACT

Host specificity is predicted to shape patterns of parasite gene flow between host species; specialist parasites should have low gene flow between host species, while generalists are predicted to have high gene flow between species. However, even for generalist parasites external forces, including ecological differences between host species may sometimes intervene to limit gene flow and create genetic structure. To investigate the potential for cryptic parasite genetic structure to arise under such circumstances, we examined the population genetic structure and history of the generalist nematode, *Trichostrongylus axei*, infecting six sympatric wild ungulate species in North America. Using genotypes for 186 *T. axei* larvae at two mitochondrial genes, *cox1* and *nad4*, we found that *T. axei* was completely panmictic across host species, with 0% of genetic variation structured between host species and 97% within individual hosts. In addition, *T. axei* showed no evidence of recent genetic bottlenecks, had high nucleotide diversities (above 2%), and an effective population size estimated to be in the tens of millions. Our result that *T. axei* maintains high rates of gene flow between multiple sympatric host species adds to a growing body of information on trichostrongylid population genetic structure in different ecological contexts. Furthermore, the high rates of gene flow, coupled with high levels of genetic diversity and large effective population size which we observed in *T. axei*, point to a potentially broad capacity for rapid evolutionary change in this parasite.

1. Introduction

Information about the genetic structure of parasite populations can be useful for understanding ecological and evolutionary processes in parasites (Nadler, 1995; Criscione et al., 2005; Barrett et al., 2008; Archie et al., 2009). For example, several recent studies have used parasite population genetics to infer aspects of parasite population history, transmission and host-parasite co-evolution, which would have otherwise been difficult to uncover (e.g. Theron et al., 2004; Wilson et al., 2005; Criscione, 2008; Criscione et al., 2010). Moreover, the structure of genetic diversity in parasite populations plays a key role in how parasite traits evolve. Hence, researchers are increasingly interested in understanding the factors involved in structuring genetic diversity in parasite populations.

Consensus is emerging that parasite life history traits, including transmission mode, life-cycle complexity and host specificity, all influence the genetic structure of parasite populations (Nadler, 1995; Blouin et al., 1999; Criscione and Blouin, 2004; Criscione et al., 2005; Barrett et al., 2008). Host specificity, in particular, can influence the genetic structure of parasites by affecting patterns of parasite gene flow between host species (Nadler, 1995; Criscione et al., 2005; Poulin and Keeney, 2008). For example, high host specificity (i.e. specialism) is predicted to limit gene flow between host species, leading to strong genetic differentiation between conspecific parasites infecting different hosts. In contrast, low host specificity (i.e. generalism) is thought to result in high gene flow between host species and few genetic differences between parasites infecting different hosts. As such, patterns of parasite genetic structure are expected to co-vary with host range; in particular, generalist parasites should show little or no genetic structuring across host species. While this prediction is supported by several studies (e.g. Sehgal et al., 2001; Brant and Orti, 2003), it is unclear how broadly this idea applies in natural host-parasite systems. This is because barriers to cross-species transmission, such as behavioral or ecological differences between host species, may limit parasite gene flow among host species, even in the presence of low host specificity (e.g. McCoy et al., 2001).

Trichostrongylid nematodes are an interesting system for exploring the population genetic consequences of generalism. As

☆ Note: Sequences in this paper were submitted to NCBI GenBank™, Accession Nos. HM744763–HM745134.

* Corresponding author at: Department of Biological Sciences, University of Notre Dame, Notre Dame, IN, USA. Tel.: +1 574 631 0178; fax: +1 574 631 7413.
E-mail address: earchie@nd.edu (E.A. Archie).

0020-7519/$36.00
doi:10.1016/j.ijpara.2010.07.014

expected for generalist parasites with low host specificity, many trichostrongylids exhibit high levels of gene flow among populations (e.g. Blouin et al., 1995; Braisher et al., 2004; Cerutti et al., 2009). However, most studies reporting these patterns have focused on parasite genetic structure across allopatric populations of single host species (e.g. Blouin et al., 1995; Braisher et al., 2004; Webster et al., 2007), leaving a gap in our understanding of trichostrongylid genetic structure when parasites infect multiple host species living in sympatry (see Brant and Orti, 2003; and Cerutti et al., 2009 for exceptions). On the one hand, these parasites might show higher rates of gene flow between sympatric host species than they do across allopatric host populations because the effects of isolation and genetic drift are probably stronger in allopatry than in sympatry. On the other hand, there may be limited parasite gene flow between sympatric host species if ecological forces reduce between-species parasite migration. For example, this latter situation might arise in host-parasite systems where spatial and/or temporal niche partitioning affects contact rates between hosts.

The potential for genetic structuring in generalist parasites might have consequences for parasite population dynamics (i.e. changes in population size over time) and evolutionary potential (i.e. the capacity of a population to experience evolutionary change). For instance, parasites with high gene flow between host species should not depend on the population dynamics of single host species and therefore should be able to maintain large effective population sizes and high evolutionary potential (Dobson, 2004; Barrett et al., 2008). However, if factors such as allopatry or niche partitioning intervene to limit gene flow in a generalist parasite, then generalists might be more dependent on the population dynamics of just one or a few host species and they might experience more frequent genetic bottlenecks, which could exacerbate cryptic genetic structure and reduce evolutionary potential (Dobson, 2004; Barrett et al., 2008).

Here we investigate the population genetic structure of a generalist nematode parasite, *Trichostrongylus axei*, across multiple species of sympatric hosts, focusing on six species of wild ungulates co-inhabiting the National Bison Range (NBR), Montana, USA. We explore between-host gene flow and its consequences for parasite evolutionary potential and population history. *T. axei* is a globally-distributed parasite of livestock, known to infect cattle, sheep, goats, pigs, horses, donkeys and rarely humans. *T. axei* also commonly infects a range of wild ungulate species (Hoberg et al., 2001). Work from related trichostrongylids suggests that this group is characterized by high rates of gene flow between allopatric host populations (e.g. Braisher et al., 2004; Webster et al., 2007). As such, our objectives were to: (i) test whether *T. axei* similarly lacks genetic differentiation across sympatric host species, or whether there is evidence of cryptic genetic structure; and (ii) examine the consequences of observed patterns of gene flow for the maintenance of stable population sizes and genetic diversity in the parasite population over time.

2. Materials and methods

2.1. Study site and host species

Nematode hosts were six ungulate species inhabiting the NBR, Moiese, Montana, USA. The NBR consists of 86 km^2 of palouse prairie and is home to a semi-managed population of approximately 350 American bison (*Bison bison*), as well as unmanaged populations of bighorn sheep (*Ovis canadensis*), elk (*Cervus elaphus*), mule deer (*Odocoileus hemionus*), white-tailed deer (*Odocoileus virginianus*), and pronghorn antelope (*Antilocapra americana*). The six species differ in their patterns of habitat use at the NBR (Ezenwa and VO, unpublished data). Bison are rotated seasonally among eight fenced pastures that partition the property; and the five other ungulate species cross the fences and move inside and outside the range at will.

2.2. Gastrointestinal (GI) nematode sampling

To sample GI nematodes, we collected fecal samples from all six ungulate host species between July and December 2007. Ungulates were located opportunistically by driving along roads that span the study site. When animals were observed defecating, we waited for them to move away and then collected fresh feces in plastic bags. Samples from bighorn sheep were collected from known individuals. For the other five host species, individuals were not distinguishable, therefore we minimized the risk of collecting multiple samples from the same individual by collecting only one sample per individual in a group and only sampling a given area once per day. In some cases, when we observed study subjects but did not observe defecation, we searched the area for fresh fecal piles. In these cases, fecal piles separated by more than 2 m were considered independent, and we never collected more samples than we observed group members. After collection, all samples were stored at 4 °C until processing. Overall we collected 335 fecal samples across all host species (Table 1).

To isolate nematode larvae, we used larval culture. Briefly, we placed 10–20 g of feces in sealed 30 ml culture jars at room temperature for 10 days. Cultures were checked every 2–3 days and stirred to prevent fungal growth. At the end of 10 days, the jars were filled with deionized H_2O, inverted on a Petri dish, and left for ~24 h. Larvae migrating into clean water in the Petri dish were examined and collected under a stereomicroscope. For each sample, we collected 200 μl of H_2O containing as many live larvae as possible into a 0.5 ml microcentrifuge tube.

2.3. DNA extraction

Larval suspensions (larvae in H_2O) were stored at 4 °C and processed for DNA extraction within 1–4 days. DNA was extracted from individual larvae following a four-step process. First, larvae were exsheathed to remove their outer cuticle by adding 9 μl of sodium hypochlorite (3.5% active Cl) to each 200 μl larval suspension and incubating at room temperature for 5 min (Coles et al., 2006). Second, to remove the sodium hypochlorite, we centrifuged the larval suspension, removed the supernatant and washed the pelleted larvae with deionized H_2O. This wash was repeated and the tube was filled with 500 μl of deionized H_2O. Third, under the stereomicroscope we collected individual, live larvae in 5 μl of deionized H_2O into separate 0.2 ml PCR tubes. To these individual larvae we added 15 μl of lysis buffer (Redman et al., 2008) containing 2 μl 10X PCR buffer (Buffer I with 15 mM $MgCl_2$, Applied Biosystems), 0.8 μl $MgCl_2$, 2 μl 4.5% Nonidet P-40, 2 μl 4.5% Tween 20, 2 μl of a 2 mg/ml solution of proteinase K and 6.2 μl H_2O. Larvae in buffer were stored at −80 °C for up to 4 months. Fourth and finally, DNA was extracted by incubating each larva in buffer at 60 °C for 98 min, then at 94 °C for 20 min. DNA extracts were diluted 1:5 and stored at −80 °C.

2.4. Genetic methods to identify T. axei

We used two genetic markers to identify *T. axei* and assemble a set of *T. axei* larvae for population genetic analysis. First, for a subset of 432 unidentified larvae (eight larvae collected randomly from nine individuals from six host species), we amplified and sequenced ~250 bp of ITS2 rRNA (Gasser et al., 1993). PCR amplification was performed in 12 μl reactions containing 1 μl of DNA extract (diluted 1:5), 0.6 μl of each 10 μM primer (NC1-ACGTCTGGTTCAGGGTTGTT; NC2-TTAGTTTCTTTT CCTCCGCT), 1.2 μl of 2 mM dNTP, 1.2 μl 10x

Table 1
Hosts and nematode larvae screened for *Trichostrongylus axei*, and the sample size of *T. axei* larvae genotyped at *nad4* and *cox1*.

Host species	Percent of fecal samples with nematode larvae	Relative prevalence of *T. axei* infection[a]	Number of *T. axei* genotyped at *nad4* and *cox1*	Number of individual hosts from which genotyped *T. axei* were collected	Average number (and range) of *T. axei* genotyped at *nad4* and *cox1* per host individual
Bighorn sheep	63% (40 of 65)	100% (21 of 21)	45	24	1.88 (1–4)
Bison	93% (50 of 54)	87% (13 of 18)	42	23	1.83 (1–5)
Elk	74% (46 of 62)	83% (15 of 18)	41	27	1.52 (1–4)
Mule deer	79% (41 of 52)	71% (12 of 17)	43	23	1.87 (1–4)
Pronghorn	91% (50 of 55)	25% (5 of 20)	1	1	1 (1)
White-tailed deer	68% (41 of 61)	67% (12 of 18)	14	8	1.75 (1–3)
Total	80% (286 of 335)	72% (78 of 109)	186	106	1.76 (1–5)

[a] Relative prevalence was calculated from a set of 2197 larvae that were sequenced at ITS2, and only included host individuals where we sequenced more than 10 larvae per individual (average number of larvae per host individual ± SD = 20.16 ± 5.93).

PCR buffer without $MgCl_2$, 0.96 μl of 1.5 mM $MgCl_2$, 0.16 μl of AmpliTaq Gold DNA polymerase (Applied Biosystems) and 5.08 μl of water. Amplification was preceded by a 10 min polymerase activation step at 95 °C, followed by 40 cycles of 45 s each at 55 °C annealing, 72 °C extension and 95 °C denaturation. These cycles were followed by a 5 min extension step at 72 °C. Positive PCR reactions were cleaned using ExoSAP and sequenced in one direction using Dye Terminator Cycle Sequencing (Applied Biosystems). The resulting ITS2 sequences were compared with template sequences in GenBank to identify *T. axei* larvae.

Second, we screened 1440 additional larvae using a *T. axei*-specific marker that amplified 72 bp of the ITS2 rRNA (Wimmer et al., 2004). PCR products were screened for the presence of a 72 bp band on agarose gels. To confirm that this marker amplified only *T. axei* in our samples, we re-amplified the subset of 432 larvae described above and found that *T. axei* was the only species to produce a 72 bp product with these primers. PCR conditions for this reaction were as follows: each 10 μl reaction contained 1 μl of DNA extract (diluted 1:5), 0.5 μl of each 10 μM primer (For-AGGGATATTAATGTCGTTCA; Rev-TGATAATTCCCATTTTAGTTT), 1 μl of 2 mM dNTP, 1 μl 10x PCR buffer without $MgCl_2$, 0.8 μl of 1.5 mM $MgCl_2$, 0.08 μl of AmpliTaq Gold DNA polymerase (Applied Biosystems) and 5.12 μl of water. Amplification was preceded by 10 min at 95 °C, followed by 40 cycles of 45 s each at 55 °C annealing, 72 °C extension and 95 °C denaturation, followed by 5 min at 72 °C.

Finally, to gain a better sense of the relative prevalence of *T. axei* across host species, we calculated the percentage of GI nematode-infected hosts that were shedding *T. axei* larvae. To do this, we used all individuals in which we had identified at least 10 larvae, and we sequenced an additional 1765 larvae using the ITS2 primers NC1 and NC2 (reaction described earlier in this section; Gasser et al., 1993). *T. axei* larvae identified using the species-specific marker were not included in prevalence estimates because this marker was applied non-randomly to maximize the number of *T. axei* sampled from different host individuals included in our population genetic analyses.

2.5. Genetic markers to characterize T. axei population genetic structure

We amplified two mitochondrial loci, NADH dehydrogenase 4 (*nad4*) and cytochrome oxidase 1 (*cox1*), from 186 *T. axei* larvae (Table 1). We amplified 655 bp of *cox1* using universal primers LCOX1490- GGTCAACAAATCATAAAGATATTGG and HCO2198-TAAACTTCAGGGTGACCAAAAAATCA (Folmer et al., 1994). For the *nad4* locus, we initially amplified a 600 bp region beginning in *cox1*, spanning the variable-length long-non-coding region, and ending in *nad4*, using P1-CGACAAACCACCTTGATATTT (Blouin et al., 1995) and P4-CARAGWGATTCHAAGKCWTTRGCAGCWTATTC (Webster et al., 2007); however these primers did not reliably amplify all *T. axei,* therefore we redesigned the P4 primer (redesignedP4-GCAGCATATTCGTCAATTACTC). Reaction conditions were identical for *nad4* and *cox1,* except for their annealing temperatures; each 12 μl reaction contained 1 μl of DNA extract (diluted 1:5), 0.6 μl of each 10 μM primer, 1.2 μl of 2 mM dNTP, 1.2 μl 10x PCR buffer without $MgCl_2$, 1 μl of 1.5 mM $MgCl_2$, 0.16 μl of AmpliTaq Gold DNA polymerase (Applied Biosystems) and 6.24 μl of water. Amplification was preceded by 10 min at 95 °C, followed by 40 cycles of 1 min at 50 °C annealing for *nad4* (or 42 °C annealing for *cox1*), 72 °C extension and 30 s 95 °C denaturation, followed by 5 min at 72 °C. Positive PCR reactions were cleaned using ExoSAP and sequenced in the 3′ and 5′ directions using Dye Terminator Cycle Sequencing (Applied Biosystems).

2.6. Analyses of DNA sequence evolution and evolutionary relationships

DNA sequences were inspected using Sequencher software version 4.1 (Gene Codes Corporation) and aligned using MEGA software version 2.1 (Kumar et al., 2001). As reported by previous authors (Blouin et al., 1995; Webster et al., 2007), the long non-coding region could not be aligned and was trimmed from all *nad4* sequences. To understand patterns of sequence evolution, we used the Akaike information criterion (AIC) in MODELTEST version 3.7 (Posada and Crandall, 1998) to choose the most likely model of evolution for *nad4* and *cox1* and the concatenated data set.

To examine the evolutionary relationships among *T. axei* haplotypes infecting different host species, we constructed statistical parsimony networks based on pair-wise differences using TCS software version 1.2.1 (Clement et al., 2000). Because the resulting networks were complex, involving multiple alternative linkages, we visualized network relationships using CYTOSCAPE version 2.6.3 (Shannon et al., 2003). Because only one *T. axei* infecting pronghorn antelope was included in the data set for population genetic analyses, this larva was included in the network but excluded from analyses of genetic variance within and between species and migration rates.

2.7. Estimates of genetic structure and gene flow across host species

To understand how genetic variation in *T. axei* was distributed within and between host species and host individuals, we used an analysis of molecular variance (AMOVA) implemented by ARLEQUIN version 3.1 (Excoffier et al., 2005). We determined the degree of correlation among genotypes using hierarchical estimates of Φ, which are analogous to Wright (1931) *F*-statistics. Specifically, we measured how variation was partitioned (i) within and between host species relative to the entire population, and (ii) within and between individual hosts in a given host species relative to other host species and the entire population. Genetic distance for AMOVA analyses was calculated using the Kimura 2-parameter model. Significance of these genetic structures was evaluated using the

permutation procedure (10,000 replicates) contained within ARELQUIN. Pairwise estimates of F_{ST} between parasites infecting different host species were generated using ARELQUIN.

2.8. Analyses of evolutionary potential and effective population size

To infer evolutionary potential, we used LAMARC software (version 2.1.3; Kuhner, 2006) to estimate Θ, which is a measure of the capacity of a population to maintain genetic diversity. We assumed that mtDNA provides an accurate reflection of population history (Avise et al., 1987; Ballard and Rand, 2005). For mtDNA, Θ equals $2N_e\mu$, where N_e is the effective population size of females and μ is the mutation rate per gene per generation. Specifically, we used LAMARCto infer Θ for each gene separately, and for a data set that included both genes together, with each gene tightly linked within the same segment. We used the growth-enabled model in LAMARC to estimate Θ because a likelihood ratio test indicated that this model provided a significantly better fit for our data than the model assuming population stasis (likelihood ratio test for the concatenated data set: $X^2 = 110.71$; d.f. = 1; $P < 0.001$). Analyses used a general time reversible (GTR) model of evolution, using the best-fitting evolutionary parameters for each gene, as chosen under the AIC criterion in MODELTEST. Each analysis used a single chain with 50,000,000 steps following an initial burn-in period of 500,000 steps. Analyses were repeated three times with different random number seeds to assess consistency. The results of these three analyses were combined in Tracer software (version 1.5) to obtain our final estimate of Θ. Estimated sample sizes were greater than 700 for each combined data set.

Our estimates of Θ from LAMARC were then used to calculate the effective population size of female *T. axei* using the equation $N_e = \Theta/2\mu$, where μ is the mutation rate per site per generation. Our estimates of μ were based on a mutation rate of 1.57×10^{-7} ($\pm 3.1 \times 10^{-8}$) substitutions per site per generation, which was directly estimated from *Caenorhabditis elegans* mtDNA (Denver et al., 2000). For each gene, and for the concatenated data set, we calculated a range of effective population sizes, for the median Θ and its upper and lower 95% posterior probability density, and for three mutation rates: 1.57×10^{-7} plus or minus 3.1×10^{-8} substitutions per site per generation (rate and confidence interval used for all subsequent analysis involving mutation rates; Denver et al., 2000).

2.9. Analyses of population history

To investigate the population history of *T. axei*, we used three methods. First, we used ARELQUIN version 3.1 (Excoffier et al., 2005) to calculate two statistics that capture genetic signatures of deviation from neutrality and population decline or expansion: Tajima's *D* (Tajima, 1989) and Fu's F_s (Fu, 1997). When a population declines, it loses rare alleles and hence the number of pair-wise differences between haplotypes is larger than expected given the number of segregating sites. When a population expands it is expected to gain rare alleles, and hence the number of pair-wise differences between sequences is smaller than expected given the number of segregating sites. Tajima's *D* and Fu's F_s capture these population signatures; we estimated these via 10,000 computer simulations based on the observed number of pair-wise differences in our samples. For both estimates, a positive value indicates a population decline and a negative value suggests a population expansion.

Tajima's *D* and Fu's F_s are susceptible to deviations from the infinite sites model of evolution. In particular, sequences with high rate heterogeneity, as is typical of nematode mtDNA (Mes, 2003), might mimic population expansions. Hence, we also inferred population history using the mismatch distribution (i.e., the distribution of the number of pair-wise differences over all sequences), which is robust to deviations from the infinite sites model (Rogers et al., 1996). When populations have experienced stable population sizes for long periods of time, the mismatch distribution is expected to be multimodal. Under expansion, the mismatch distribution is expected to be unimodal and bell-shaped, without large differences in the frequency of ranked pair-wise differences in the population (also known as a low raggedness, *R*). Mismatch distributions were analyzed in ARELQUIN (Rogers and Harpending, 1992; Rogers, 1995; Schneider and Excoffier, 1999; Excoffier, 2004; Excoffier et al., 2005). Specifically, we assessed the goodness-of-fit of the observed data to the predicted distribution for an expanded population for 10,000 simulations using a sum of squares (SSD) method. When the observed distribution fits the expansion model, then $P \geqslant 0.05$. We also estimated the time to the most recent common ancestor (TMRCA) of our sequences, which can be used to approximate the number of generations since a population expansion (t). Specifically, t can be estimated from the peak distribution (τ; the time since the expansion in units of N_e generations) as $t = \tau/2\mu$ (re-arranged from Li, 1977), where μ is the mutation rate per gene per generation. We obtained this by multiplying the mutation rate per site per generation, 1.57×10^{-7} ($\pm 3.1 \times 10^{-8}$), by the number of nucleotides in each gene. From our estimate of t we calculated the approximate number of years since the expansion, by dividing t by the number of generations per year. Generation times for trichostrongylid nematodes are not well known, so we estimated possible maximum and minimum generation times for *T. axei* based on what is known about trichostrongylid life histories. We calculated the maximum generation time as eight generations per year using an estimated time from egg to egg-laying adult of 31 days (*Trichostrongylus* spp. prepatent period of ~21 plus ~10 days for egg hatching, larval development and infection (Douvres, 1957; Audebert et al., 2003)), multiplied by a breeding season of 8 months per year (April–November; Crofton, 1954, 1957 in southwestern England). This maximum estimate assumes a relatively long breeding season and the minimum possible time for egg hatching, larval development and infection. However, a number of environmental and host-related factors can delay these processes (e.g., Young and Anderson, 1981; Michel, 1970; reviewed in O'Connor et al., 2006), thus we estimated a minimum generation time of one to two generations per year based on the observation that trichostrongylid infective larvae sometimes require up to 3–6 months to develop from egg to mature adult (Young and Anderson, 1981; Michel, 1970; O'Connor et al., 2006). Such a developmental rate could produce as few as one to two generations per year.

Third and finally, we used the Bayesian Markov Chain Monte Carlo (MCMC) method implemented in BEAST software (version 1.5.2, Drummond and Rambaut, 2007) to infer changes in the population size of *T. axei* over time. We performed these analyses on a data set that combined both *nad4* and *cox1* data sets, implementing the substitution gene-specific models obtained under the AIC criterion in MODELTEST. Specifically, we used BEAST to infer the TMRCA of each data set, and the demographic history of these lineages using Bayesian skyline plots (BSP). The BSP demographic model is ideal because it can fit a wide range of demographic scenarios and accommodate deviations from the infinite sites model (Drummond and Rambaut, 2007). We compared estimates inferred using a strict molecular clock with those using the relaxed clock option with uncorrelated, log-normal branch-specific rates. The MCMC analyses were first performed with short chain lengths (10^6 or 10^7) to optimize parameters. Final analyses were run with the strict molecular clock option and a mutation rate of 1.57×10^{-7} per site per year for 50 million iterations, sampling every 1000th iteration after a burn-in period of 5 million steps (10% of 50 million). The performance of the MCMC processes were checked for

stationarity and large effective populations sizes in TRACER software (version 1.5.2, Drummond and Rambaut, 2007).

3. Results

3.1. Patterns of T. axei infection across host species

We collected 335 fecal samples across six host species and recovered GI nematodes from over 60% of all samples from each host species (Table 1). Among animals infected with GI nematodes, the relative prevalence of *T. axei* ranged from 25% to 100% across host species. Pronghorn was the only host species in which *T. axei* occurred in fewer than half of nematode-infected individuals (Table 1).

3.2. Patterns of mitochondrial DNA evolution

For 186 *T. axei* collected across all six host species, we sequenced and aligned 655 bp of the *cox1* region and 477 bp of *nad4* (Table 1; GenBank Accession Nos. HM744763–HM745134). MODEL TEST indicated that patterns of sequence evolution in both *cox1* and *nad4* were similar; both *cox1* and *nad4* were AT rich, with high transition/transversion ratios and fairly substantial rate heterogeneity (Supplementary Table S1). The best model of evolution for *cox1* was TIM + I + G, while the best model of evolution for *nad4* was K81uf + I + G. Both models incorporate unequal base frequencies and rate heterogeneity, with two different transversion rates, but they differ in that K81uf has one rate for all transition types, while TIM has two rates for transitions.

3.3. Gene flow across host species

Statistical parsimony networks of *cox1* and *nad4* haplotypes revealed that *T. axei* haplotypes grouped into two clades, which were not correlated with host species (Fig. 1). Haplotypes from different host species were randomly distributed across the network, with no evidence for genetic structuring within host species. Furthermore, rates of gene flow between species were high enough that *T. axei* appeared to be a single panmictic population; an AMOVA of *cox1* and *nad4* haplotypes revealed that 100% of the genetic variation in *T. axei* was contained within the populations infecting

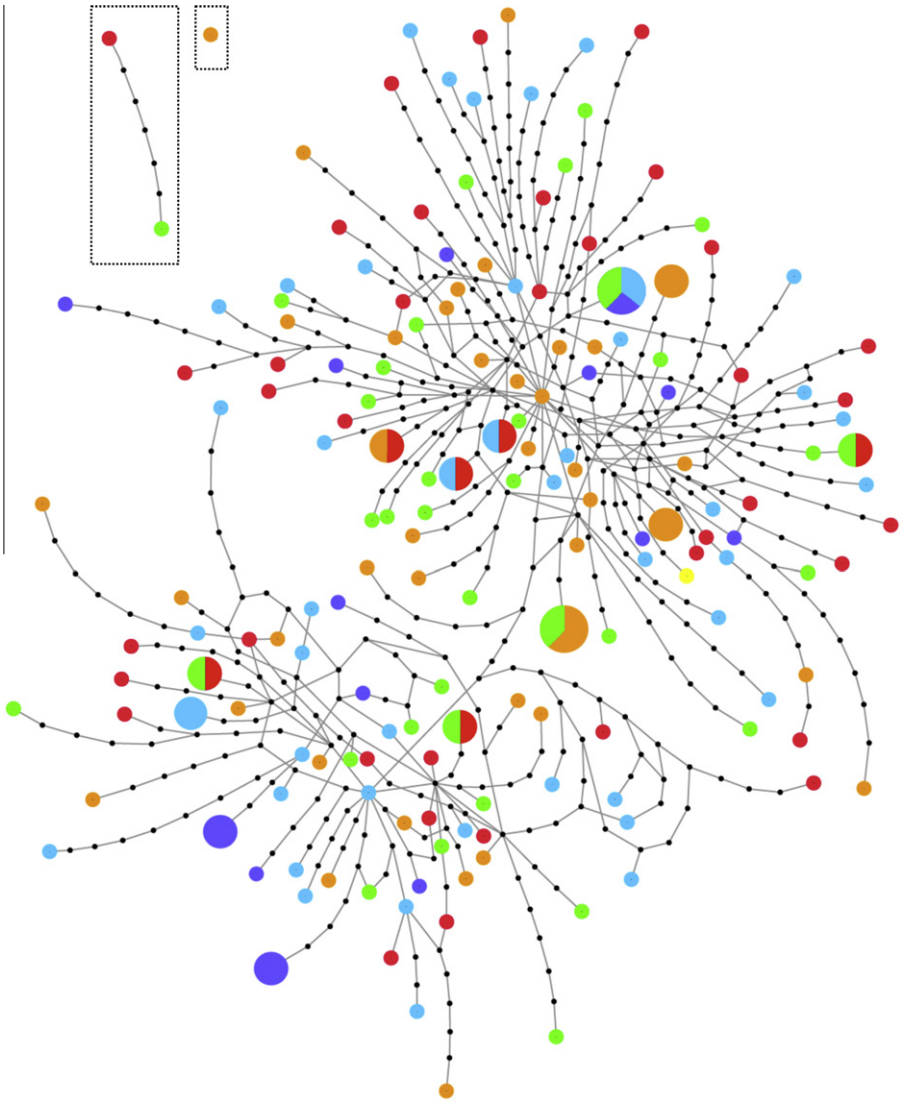

Fig. 1. Statistical parsimony network of concatenated *nad4* haplotypes from 186 *Trichostongylus axei* collected from six different host species. Results for *cox1* (not shown) were similar. Black dots indicate mutational steps separating haplotypes. Colored circles represent *nad4* haplotypes found infecting each host species (light blue = bighorn sheep, red = bison, green = elk, orange = mule deer, purple = white-tailed deer and yellow = pronghorn). Haplotype frequency is represented by the size of the circle; the smallest circles contain one haplotype, the largest circles contain three haplotypes. The haplotypes in dashed boxes did not connect with ⩾95% confidence anywhere in the network.

each host species, while 0% occurred between host species (Table 2). In fact, the vast majority of genetic variation within the *T. axei* population occurred in individual host animals, as 97% of the variation in the *T. axei* population was reflected in the larvae infecting individual hosts (Table 2). Φ_{ST} between *T. axei* infecting different host species was −0.005, which was not significantly different from zero. This lack of genetic differentiation between larvae infecting different host species persisted when we considered genetic differentiation between all possible pairs of species; no pair-wise Φ_{ST} values were significantly different from zero (Table 3).

3.4. Genetic diversity and effective population size

Levels of sequence diversity were high in *T. axei*; 87% (161 of 186) of concatenated haplotypes were unique and the average nucleotide diversity (π) was greater than 2% for both genes (average number of pair-wise differences between haplotypes; *nad4* = 12.4, *cox1* = 15.7). Furthermore, we found that the median estimates of Θ in *T. axei* ranged from 10.32 to 15.28 across both genes and the concatenated data set (Table 4). These values indicate that *T. axei* has a large effective population size and capacity to maintain genetic diversity. Specifically, assuming the mutation rate of Denver et al. (2000), we estimated the effective population size of female *T. axei* to be in the tens of millions (Table 4).

3.5. Population history

We found genetic evidence that *T. axei* experienced a substantial population expansion. Tajima's D and Fu's F_s for both *nad4* and *cox1* were strongly and significantly negative (Tajima's D: *cox1* = −1.46, $P = 0.035$; *nad4* = −2.01, $P = 0.002$; Fu's Fs: *cox1* = −23.81, $P = 0.002$; *nad4* = −24.11, $P = 0.001$). In addition, as expected under population expansion, the mismatch distributions of both *cox1* and *nad4* were not significantly different from unimodal (*cox1* $P = 0.21$, *nad4* $P = 0.48$; Fig. 2), and raggedness indices were low (*cox1* $R = 0.001$, $P = 0.99$; *nad4* $R = 0.002$, $P = 0.94$). As population expansions become more ancient, the mean and mode of the mismatch distribution increases, and hence mismatch distributions can also be used to date population expansions. The peak of the unimodal distributions (τ) was 18.31 for *cox1* and 11.73 for *nad4*, corresponding to a population expansion approximately 85,000 generations ago (~85,000 years ago, assuming one generation per year; ~40,000 years ago assuming two generations per year; ~10,000 years ago assuming eight generations per year; Table 5).

TMRCA calculations derived from the mismatch distribution assume that the *T. axei* population is at equilibrium, and the fact that this population has experienced an expansion violates this assumption. Therefore, to obtain an independent estimate of *T. axei* population history, we used the Bayesian MCMC sampling procedures implemented in BEAST software to estimate the posterior distribution of the TMRCA and the effective population size through time. The posterior means of the TMRCA estimates were similar under the strict or relaxed molecular clock models (Supplementary Fig. S1), and the results were similar to population histories inferred from the mismatch distribution. The TMRCA was estimated to be approximately 200,000 generations ago (95% highest posterior density = 154,000–247,000 generations; Supplementary Fig. S1). The demographic reconstructions from Bayesian skyline plots indicate that the *T. axei* population began to expand approximately 100,000 generations ago, reaching a peak expansion rate around 75,000 generations ago, and reaching stasis around 50,000 generations ago (Fig. 3).

4. Discussion

We investigated the genetic structure of *T. axei*, collected from six sympatric species of wild ungulates. Our aim was to better understand parasite population genetic structure in a context where a single parasite infects multiple, co-occurring host species. All six ungulates were infected with *T. axei*, and using parasite larvae shed by individuals of each of these host species, we found no evidence of cryptic parasite genetic structure. Instead, *T. axei* was completely panmictic across host species and 100% of the population-wide genetic variation in *T. axei* occurred in each host species. When we included the individual level of analysis, 97% of the population-wide genetic variation occurred within individual hosts, compared with 3% within host species. Furthermore, statistical parsimony networks of *cox1* and *nad4* haplotypes revealed that *T. axei* haplotypes clustered into two clades that were not correlated with host species (Fig. 1), providing further evidence of a lack of cryptic structure associated with host use. A number of studies on other trichostrongylid nematodes have found high rates of gene flow between allopatric host populations (e.g. Blouin et al., 1995; Braisher et al., 2004; Webster et al., 2007; Cerutti et al., 2009), and the high gene flow between host species we report in *T. axei* suggests that this feature may be broadly characteristic of generalist trichostrongylids. Moreover, the partitioning of genetic variation in *T. axei* was also concordant with findings from other trichostronglyids. For example, Webster et al. (2007) also found that 97% of the total genetic variation in their sample of *Trichostrongylus tenuis* was structured within individual hosts. The presence of two distinct mtDNA clades has been described for another trichostrongylid, *Haemonchus contortus* (Cerutti et al., 2009). Thus, the two clades we found in *T. axei* may reflect a genetic division that occurred prior to the arrival of *T. axei* in North America, and may be indicative of similarities in the population history of *T. axei* and related nematodes such as *H. contortus*.

Although our results support the generalization that low host specificity is linked to high gene flow between host species, under certain conditions ecological forces can lead to genetic structuring in generalist parasites. For instance, for the generalist tick, *Ixodes uriae*, McCoy et al. (2001) found greater genetic differentiation between ticks from different sympatric host species than between ticks from neighboring allopatric populations of the same host species. They attributed this pattern to a number of ecological factors, including differences in host phenology (McCoy et al., 2001). The six host species we considered in our study, although sympatric, are known to utilize habitat in different ways (Singer and Norland, 1994). At the NBR specifically, habitat overlap between pairs of ungulate species ranges from 0 to 42% (Ezenwa, VO, unpublished data), suggesting that there was some degree of spatial niche partitioning between hosts in our study. Nevertheless, host ecology appeared to be insufficient to create significant barriers to parasite migration between species. One possible explanation for this lack of an effect could be that the persistence of *T. axei* infective stages in the environment facilitates cross-species parasite transmission, even in the face of moderate levels of host niche partitioning. In addition, our results do not preclude the existence of finer-scale genetic structure in *T. axei* because the mtDNA loci we used might be less sensitive than unlinked microsatellite genotypes or amplified fragment length polymorphisms (AFLPs) for revealing fine-scale genetic structure. However, microsatellites are currently not well developed for most trichostrongylids (Grillo et al., 2006; Johnson et al., 2006), and AFLPs present challenges when using template DNA from non-invasively collected trichostrongylid larvae.

The high gene flow we observed in *T. axei* should have consequences for parasite population dynamics and evolutionary potential (Nadler 1995; Barrett et al., 2008). For instance, parasites with high gene flow between host species might be less likely to expe-

Table 2
Analysis of molecular variance (AMOVA) results describing how genetic differentiation is partitioned among *Trichostrongylus axei* infecting five different host species, excluding and including the proportion of genetic variation contained within individual hosts.

Source of variation	d.f.	Sum of squares	% of variation	Φ	*P*
Excluding individual host level					
Among host species	4	0.049	−0.50	−0.005	0.842
Within host species	180	2.698	100.50	0.015	NA
Including individual host level[a]					
Among host species	4	0.048	−0.69	−0.007	0.910
Among individual hosts within species	100	1.538	3.39	0.034	0.146
Within individual hosts	80	1.160	97.30	0.015	0.172

P values were obtained by comparisons of observed values with those generated by 10,000 random permutations in ARLEQUIN (version 3.1). d.f. represents the degrees of freedom in each analysis. NA is not applicable; no statistical test was performed at this level of genetic structure.
[a] Individual hosts from which only one larva was genotyped are excluded from this level of analysis.

Table 3
Pairwise F_{ST} between the populations of *Trichostrongylus axei* infecting different host species.

Pairwise comparison	F_{ST}	*P*	Pairwise genetic differences within and between parasite populations
Bighorn–bison	−0.0055	0.742	−0.00017
Bighorn–elk	0.0013	0.298	0.00004
Bighorn–muledeer	−0.0007	0.387	−0.00002
Bighorn–white-tailed deer	−0.0143	0.827	−0.00037
Bison–elk	−0.0046	0.684	−0.00014
Bison–mule deer	−0.0056	0.745	−0.00016
Bison–white-tailed deer	−0.0102	0.718	−0.00027
Elk–mule deer	−0.0072	0.839	−0.00021
Elk–white-tailed deer	−0.0145	0.841	−0.00039
Mule deer–white-tailed deer	−0.0062	0.528	−0.00018

P values indicate the probability that F_{ST} is significantly different from zero and were obtained by comparisons of observed values with those generated by 10,000 random permutations in ARLEQUIN (version 3.1). Negative pairwise genetic differences between species indicate more nucleotide differences between parasites infecting the same host species than different host species.

Table 4
Estimates of female effective population size (N_{ef}) rounded to the nearest million.

Gene	Estimates of Θ	N_{ef} ($\mu = 1.26 \times 10^{-7}$)	N_{ef} ($\mu = 1.57 \times 10^{-7}$)	N_{ef} ($\mu = 1.87 \times 10^{-7}$)
nad4				
95% lower Θ	5.05	20,000,000	16,000,000	13,000,000
Median Θ	10.32	41,000,000	33,000,000	28,000,000
95% upper Θ	18.19	72,000,000	58,000,000	49000,000
cox1				
95% lower Θ	6.09	24,000,000	19,000,000	16,000,000
Median Θ	11.79	47,000,000	38000,000	32,000,000
95% upper Θ	18.65	74,000,000	60,000,000	50,000,000
Concatenated				
95% lower Θ	8.47	34,000,000	27,000,000	23,000,000
Median Θ	15.29	61,000,000	49,000,000	41,000,000
95% upper Θ	24.73	98,000,000	79,000,000	66000,000

Estimates of female effective population size (N_{ef}), via the equation $N_{ef} = \theta/2\mu$ where μ is the mutation rate per site per generation ($1.57 \times 10^{-7} \pm 3.1 \times 10^{-8}$ from Denver et al. (2000)).

rience population bottlenecks because they depend on multiple host species. Congruent with this expectation, our results indicate that *T. axei* has not experienced a recent population bottleneck. In fact, we found evidence suggestive of a population expansion in *T. axei* between 10,000 and 40,000 years ago. Although caution should be used when interpreting these results because mtDNA mutation patterns could mimic the departure from neutrality expected under demographic expansion, similar patterns of population expansion have been described for several other parasitic nematodes (Mes, 2003; Morrison and Hoglund, 2005). Previous researchers have proposed that these population expansions were caused by expansions in human-associated animals (i.e. livestock hosts) over the last 10,000 years (Mes, 2003; Morrison and Hoglund, 2005). Archeological and genetic data indicate that livestock populations did expand in the last 10,000 years (Finlay et al., 2007). Moreover, in temperate regions, several species of wild ungulate hosts also experienced population expansions approximately 10,000 years ago (e.g. Flagstad and Roed, 2003; Lessa et al., 2003; Sommer et al., 2008). If our most recent estimate for *T. axei*'s population expansion (~10,000 years ago; Table 5) best reflects the population history of *T. axei*, then the observed population expansion in *T. axei* could have been driven by changes in the population sizes of both its wild and domesticated hosts. Using a slower, more conservative, generation time of one to two generations per year produces a population expansion estimate of ~40,000–85,000 years ago (Table 5). If this estimate more accurately reflects the population history of *T. axei*, then it is unlikely that population expansion of this parasite was caused by expansions in either livestock or wild ungulate hosts. However, it is difficult to guess what might have caused such a massive expansion

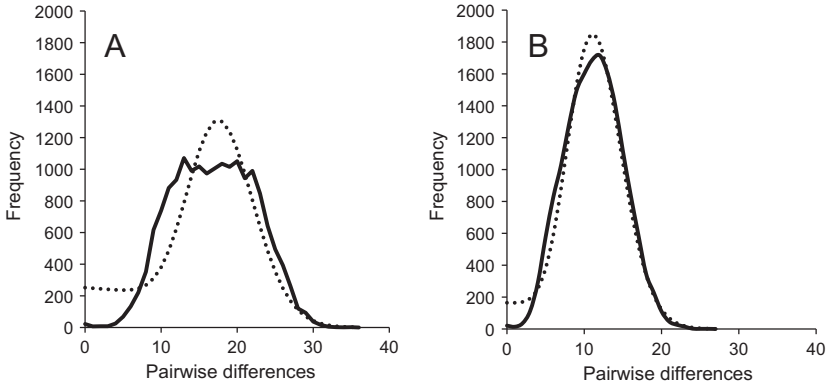

Fig. 2. Mismatch distributions of mitochondrial *cox1* (A) and *nad4* (B) genes in *Trichostrongylus axei*. Solid lines indicate the frequency pairs of sequences as a function of the number of pair-wise differences between those sequences. Dashed lines indicate a generalized non-linear least squares approximation of the expected mismatch distribution under a model of rapid population expansion.

Table 5
The time to the most recent common ancestors (TMRCA) of *cox1* and *nad4* sequences in *Trichostrongylus axei*, derived from their mismatch distributions.

Gene	τ (range $P = 0.05$)	μ	t in generations	TMRCA in years (2 generations per year)	TMRCA in years (8 generations per year)
cox1	18.31 (12.45–22.03)	1.7×10^{-4}	108,000 (73,000–130,000)	54,000 (37000–65,000)	13,000 (9,000–16,000)
		2.1×10^{-4}	89,000 (61, 000–107,000)	45,000 (30,000–54,000)	11,000 (8000–13,000)
		2.4×10^{-4}	76,000 (52,000–92,000)	38000 (26000–46,000)	10,000 (6,000–11,000)
nad4	11.73 (8.31–13.90)	1.24×10^{-4}	95,000 (67,000–112,000)	47,000 (34,000–56,000)	10,000 (7,000–11,000)
		1.50×10^{-4}	78,000 (55,000–93,000)	39,000 (28,000–46,000)	12,000 (8,000–14,000)
		1.82×10^{-4}	64,000 (46,000–76,000)	32,000 (23,000–38,000)	8,000 (6,000–10,000)

The peak mismatch distribution (τ), the mutation rate per gene per generation (μ) based on the mutation rate per site per generation ($1.57 \times 10^{-7} \pm 3.1 \times 10^{-8}$ from Denver et al. (2000)), the number of generations since the MRCA (t) from the peak distribution (τ) as $t = \tau/2\mu$ (re-arranged from Li (1977)), and the TMRCA in years, calculated by dividing t by 12.

in *T. axei* 40,000–85,000 years ago since this time period falls in the midst of the last ice age, and climate warming did not begin until approximately 15,000 years ago (Severinghaus and Brook, 1999; Denton et al., 2010).

Regardless of the timing or cause of population expansion in *T. axei*, our data strongly suggest that *T. axei* has maintained a large effective population size for an extended period of time. Large populations are expected for parasites with high gene flow between host species and our data indicate that the current effective population size of *T. axei* is in the tens of millions. This estimate is based on a mutation rate for *Caenorhabditis elegans*, and one caveat is that we assume that *C. elegans* and *T. axei* have similar mtDNA mutation rates. In support of this assumption, our estimate of N_e is concordant with Blouin et al. (1992), who estimated N_e for *Ostertagia ostertagi* to be 4–8 million in cattle from five farms across North America. The maintenance of such a large N_e in *T. axei* could be facilitated by its ability to exploit multiple wild ungulate host populations. Furthermore, the extensive gene flow we observed probably means that the parasite population extends over a relatively large spatial scale–probably much larger than our study site. If this is the case, the large effective population size of *T. axei* is likely supported by both the wild ungulate species we focused on in our study and domestic host species that are also prevalent in the region. Finally, as expected for a population that has maintained a large effective population size for a relatively long time, *T. axei* had high genetic diversity. In our study, we found that the majority of *T. axei* larvae (87%) had unique *nad4* and *cox1* haplotypes, and the average number of pair-wise differences between *nad4* and *cox1* haplotypes was 12.4 and 15.7, respectively. These values translate into nucleotide diversities greater than 2% in both *nad4* and *cox1*, which is similar to other trichostrongylid nematodes, including *O. ostertagi, Oesophagostomum bifurcum*, *H. contortus*, and *Mazamastrongylus odocoilei* (Blouin, 1998; Blouin et al., 1998; Dame et al., 1993; De Gruijter et al., 2002).

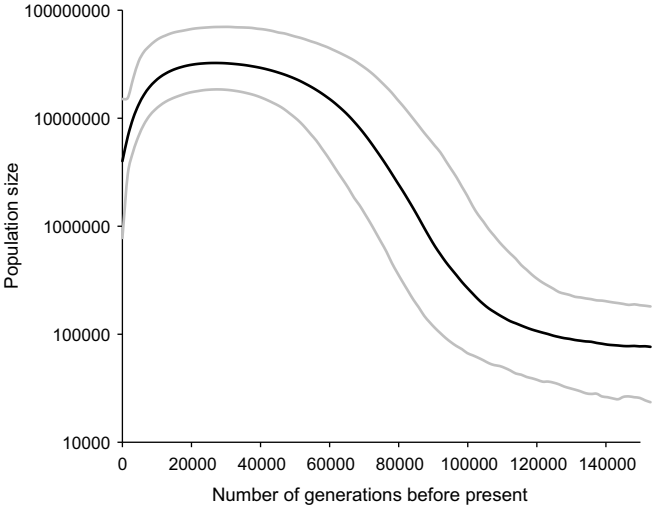

Fig. 3. Bayesian skyline plot of the change in effective population size of *Trichostrongylus axei* over time The x-axis is in units of generations before the present, and the y-axis is on a log scale and is equal to $N_e\tau$ (the product of the effective population size and the generation time). The black line is the median estimate of $N_e\tau$ and the gray lines indicate the 95% highest and lowest posterior density limits of $N_e\tau$. The presented Bayesian skyline plot was based on an analysis that assumed a relaxed molecular clock and a mutation rate of 1.57×10^{-7} mutations per site per year. Analyses assuming a strict molecular clock gave similar results.

The population genetic structure we observed in *T. axei* – high gene flow, high genetic diversity and a large effective population

size – has at least two important evolutionary consequences. First, the high rates of gene flow we observed between *T. axei* infecting different host species creates the potential for parasite genes to spread rapidly from one host population to another. Second, the large effective population size of *T. axei* and high genetic diversity mean that this parasite is able to respond efficiently to forces of selection. For alleles under selection in *T. axei*, the action of genetic drift should be negligible compared with the action of natural selection. Given the equation $N_e s \gg 1$, where s is the selection coefficient, even very small selection coefficients should be able to drive evolutionary change in *T. axei* populations.

These evolutionary consequences have implications for parasite management and the evolution of parasite traits. For instance, anthelmintic drug resistance is a costly problem for the management of many trichostrongylid nematodes, and large effective population sizes and high genetic diversity are often implicated in the rapid evolution of resistance in these species (Prichard, 1994; Kaplan, 2004). Resistance is actually less common in *T. axei* than in other trichostrongylid nematodes (Kaplan, 2004; Palcy et al., 2010), but our results indicate that evolutionary potential should not be a limiting factor in the evolution of resistance in this species. One explanation for the lower resistance in *T. axei* has been that this parasite is less common in livestock, and therefore does not experience strong selection for resistance compared with some of the most resistant nematodes, including *H. contortus*, *Teladorsagia circumcincta, Cooperia oncophora* and *Trichostrongylus colubriformis* (Kaplan, 2004; Palcy et al., 2010). Another possible explanation for lower rates of resistance in *T. axei* might be that this species experiences a release from selection because in addition to infecting livestock, it also commonly infects wildlife. When all parasite populations are under selection, as is the case for parasitic nematodes that primarily infect livestock, gene flow between populations will accelerate the movement of resistance genes and the spread of resistance between populations. However, when a nematode species commonly infects wildlife, high rates of gene flow from wild to domesticated host populations might dilute selection for resistance. At the NBR for example, surrounding cattle populations are infected with *T. axei* as well as other nematode species known to have higher rates of resistance, including *C. oncophora, H. contortus* and *O. ostertagi* (Archie, E and Ezenwa, VO, unpublished data). Of these four nematode species, *T. axei* is by far the most prevalent in wild ungulates at NBR, with an average prevalence of 79% compared with less than 50% (range: 21–47%) for the other species. This suggests that the opportunity for parasite gene flow between wild and domesticated populations might be higher for *T. axei* compared with other GI nematodes, supporting the dilution hypothesis. Future work on this topic will be key for testing the validity of this hypothesis, and for examining a possible role for wildlife in mitigating the spread of nematode resistance genes in livestock.

In conclusion, our results largely support those of other studies on the genetic structure of trichostrongylid nematode populations. We found no evidence for cryptic genetic structure in *T. axei* infecting six sympatric host species; rather *T. axei* was completely panmictic across hosts with high genetic diversity within host specific populations and within host individuals. Moreover, as predicted for a generalist parasite with high gene flow, we found a population history lacking genetic bottlenecks, a large effective population size and high evolutionary potential. This population genetic structure should impact the evolution of parasite traits. Specifically, *T. axei* should respond efficiently to selection pressure, thus genes implicated in resistance or virulence may move quickly between host species. In general, trichostrongylids appear to have very similar life histories and consequently similar genetic structures, however future work using more powerful genetic markers may reveal subtle differences between species.

Acknowledgements

We thank the National Bison Range, MT, USA for permission to conduct research and invaluable assistance. J. Hogg (Montana Conservation Science Institute, USA) provided bighorn sheep samples; and L. Fishman and S. Miller generously allowed access to equipment. This work was supported by funds from the University of Montana, USA to VOE.

Appendix A. Supplementary data

Supplementary data associated with this article can be found, in the online version, at doi:10.1016/j.ijpara.2010.07.014.

References

Archie, E.A., Luikart, G., Ezenwa, V.O., 2009. Infecting epidemiology with genetics: a new frontier in disease ecology. Trends Ecol. Evol. 24, 21–30.

Audebert, F., Cassone, J., Kerboeuf, D., Durette-Desset, M.C., 2003. Development of *Trichostrongylus colubriformis* and *Trichostrongylus vitrinus*, parasites of ruminants in the rabbit and comparison with *Trichostrongylus retortaeformis*. Parasitol. Res. 90, 57–63.

Avise, J.C., Arnold, R.M., Ball, R.M., Bermingham, E., Lamb, T., Neigel, J.E., Reeb, C.A., Saunders, N.C., 1987. Intraspecific phylogeography: the mitochondrial DNA bridge between population genetics and systematics. Annu. Rev. Ecol. Evol. Syst. 18, 489–522.

Ballard, J.W.O., Rand, D.M., 2005. The population biology of mitochondrial DNA and its phylogenetic implications. Annu. Rev. Ecol. Evol. Syst. 36, 621–642.

Barrett, L.G., Thrall, P.H., Burdon, J.J., Linde, C.C., 2008. Life history determines genetic structure and evolutionary potential of host–parasite interactions. Trends Ecol. Evol., 678–685.

Blouin, M.S., 1998. Mitochondrial DNA diversity in nematodes. J Helminthol. 72, 285–289.

Blouin, M.S., Dame, J.B., Tarrant, C.A., Courtney, C.H., 1992. Unusual Population-Genetics of a Parasitic Nematode - Mtdna Variation within and among Populations. Evolution 46, 470–476.

Blouin, M.S., Yowell, C.A., Courtney, C.H., Dame, J.B., 1995. Host movement and the genetic structure of populations of parasitic nematodes. Genetics 141, 1007–1014.

Blouin, M.S., Yowell, C.A., Courtney, C.H., Dame, J.B., 1998. Substitution bias, rapid saturation, and the use of mtDNA for nematode systematics. Mol. Biol. Evol. 15, 1719–1727.

Blouin, M.S., Liu, J., Berry, R.E., 1999. Life cycle variation and the genetic structure of nematode populations. Heredity 83, 253–259.

Braisher, T.L., Gemmell, N.J., Grenfell, B.T., Amos, W., 2004. Host isolation and patterns of genetic variability in three populations of *Teladorsagia* from sheep. Int. J. Parasitol. 34, 1197–1204.

Brant, S.V., Orti, G., 2003. Evidence for gene flow in parasitic nematodes between two host species of shrews. Mol. Ecol. 12, 2853–2859.

Cerutti, M.C., Citterio, C.V., Bazzocchi, C., Epis, S., D'Amelio, S., Ferrari, N., Lanfranchi, P., 2009. Genetic variability of *Haemonchus contortus* (Nematoda: Trichostrongyloidea) in alpine ruminant host species. J. Helminthol. 83, 276–283.

Clement, M., Posada, D., Crandall, K.A., 2000. TCS: a computer program to estimate gene genealogies. Mol. Ecol. 9, 1657–1660.

Coles, G.C., Jackson, F., Pomroy, W.E., Prichard, R.K., von Samson-Himmelstjerna, G., Silvestre, A., Taylor, M.A., Vercruysse, J., 2006. The detection of antihelminthic resistance in nematodes of veterinary importance. Vet. Parasitol. 136, 167–185.

Criscione, C.D., 2008. Parasite co-structure: broad and local scale approaches. Parasite 15, 439–443.

Criscione, C.D., Blouin, M.S., 2004. Life cycles shape parasite evolution: comparative population genetics of salmon trematodes. Evolution 58, 198–202.

Criscione, C.D., Poulin, R., Blouin, M.S., 2005. Molecular ecology of parasites: elucidating ecological and microevolutionary processes. Mol. Ecol. 14, 2247–2257.

Criscione, C.D., Anderson, J.D., Sudimack, D., Subedi, J., Upadhayay, R.P., Jha, B., Williams, K.D., Williams-Blangero, S., Anderson, T.J.C., 2010. Landscape genetics reveals focal transmission of a human macroparasite. PLOS Negl. Trop. Dis. 4, e665.

Crofton, H.D., 1954. Nematode parasite populations in sheep on lowland farms. 1. Worm egg counts in ewes. Parasitology 44, 465–477.

Crofton, H.D., 1957. Nematode parasite populations in sheep on lowland farms III. The seasonal incidence of species. Parasitology 47, 304–318.

Dame, J.B., Blouin, M.S., Courtney, C.H., 1993. Genetic Structure of Populations of *Ostertagia ostertagi*. Vet. Parasitol. 46, 55–62.

de Gruijter, J.M., Polderman, A.M., Zhu, X.Q., Gasser, R.B., 2002. Screening for haplotypic variability within *Oesophagostomum bifurcum* (Nematoda) employing a single-strand conformation polymorphism approach. Mol. Cell. Probe. 16, 185–190.

Denton, G.H., Anderson, R.F., Toggweiler, J.R., Edwards, R.L., Schaefer, J.M., Putnam, A.E., 2010. The last glacial termination. Science 328, 1652–1656.
Denver, D.R., Morris, K., Lynch, M., Vassilieva, L.L., Thomas, W.K., 2000. High direct estimate of the mutation rate in the mitochondrial genome of *Caenorhabditis elegans*. Science 289, 2342–2344.
Dobson, A., 2004. Population dynamics of pathogens with multiple host species. Am. Nat. 164, S64–S78.
Douvres, F.W., 1957. The morphogenesis of the parasitic stages of *Trichostrongylus axei* and *Trichostrongylus colubriformis*, nematode parasites of cattle. Proc. Helminthol. Soc. Wash. 24, 4–14.
Drummond, A.J., Rambaut, A., 2007. BEAST: Bayesian evolutionary analysis by sampling trees. BMC Evol. Biol. 7, 214.
Excoffier, L., 2004. Patterns of DNA sequence diversity and genetic structure after a range expansion: lessons from the infinite-island model. Mol. Ecol. 13, 853–864.
Excoffier, L., Laval, G., Schneider, S., 2005. Arlequin ver. 3.0: An integrated software package for population genetics data analysis. Evol. Bioinform. Online 1, 47–50.
Finlay, E.K., Gaillard, C., Vahidi, S.M.F., Mirhoseini, S.Z., Jianlin, H., Qi, X.B., El-Barody, M.A.A., Baird, J.F., Healy, B.C., Bradley, D.G., 2007. Bayesian inference of population expansions in domestic bovines. Biol. Lett. 3, 449–452.
Flagstad, O., Roed, K.H., 2003. Refugial origins of reindeer (*Rangifer tarandus* L.) inferred from mitochondrial DNA sequences. Evolution 57, 658–670.
Folmer, O., Black, M., Hoeh, W., Lutz, R., Vrijenhoek, R., 1994. DNA primers for amplification of mitochondrial cytochrome c oxidase subunit I from diverse metazoan invertebrates. Mol. Mar. Biol. Biotechnol. 3, 294–297.
Fu, Y.X., 1997. Statistical tests of neutrality of mutations against population growth, hitchhiking and background selection. Genetics 147, 915–925.
Gasser, R.B., Chilton, N.B., Hoste, H., Beveridge, I., 1993. Rapid sequencing of rDNA from single worms and eggs of parasitic helminths. Nucleic Acids Res. 21, 2525–2526.
Grillo, V., Jackson, F., Gilleard, J.S., 2006. Characterization of *Teladorsagia circumcincta* microsatellites. Mol. Biochem. Parasitol. 148, 181–189.
Hoberg, E.P., Kocan, A.A., Rickard, L.G. 2001. Gastrointestinal strongyles in wild ruminants. In: W.M.Samuel, M.J. Pybus, A.A. Kocan, (Eds.), Parasiticdiseases of wild mammals. Iowa State University, Ames, USA, pp. 193–227.
Johnson, P.C.D., Webster, L.M.I., Adam, A., Buckland, R., Dawson, D.A., Keller, L.F., 2006. Abundant variation in microsatellites of the parasitic nematode *Trichostrongylus tenuis* and linkage to a tandem repeat. Mol. Biochem. Parasitol. 148, 210–218.
Kaplan, R.M., 2004. Drug resistance in nematodes of veterinary importance. a status report. Trends Parasitol. 20, 477–481.
Kuhner, M., 2006. LAMARC 2.0: Maximum likelihood and Bayesian estimation of population parameters. Bioinformatics 22, 768–770.
Kumar, S., Tamura, K., Jakobsen, I.B., Nei, M., 2001. MEGA2: molecular evolutionary genetics analysis software. Bioinformatics 17, 1244–1245.
Lessa, E.P., Cook, J.A., Patton, J.L., 2003. Genetic footprints of demographic expansion in North America, but not Amazonia, during the Late Quaternary. Proc. Natl. Acad. Sci. USA 100, 10331–10334.
Li, W.H., 1977. Distribution of nucleotide differences between two randomly chosen cistrons in a finite population. Genetics 85, 331–337.
McCoy, K.D., Boulinier, T., Tirard, C., Michalakis, Y., 2001. Host specificity of a generalist parasite: genetic evidence of sympatric host races in the seabird tick *Ixodes uriae*. J. Evol. Biol. 14, 395–405.
Mes, T.H., 2003. Demographic expansion of parasitic nematodes of livestock based on mitochondrial DNA regions that conflict with the infinite-sites model. Mol. Ecol. 12, 1555–1566.
Michel, J.F., 1970. The regulation of populations of *Ostertagia ostertagi* in calves. Parasitology 61, 435–447.
Morrison, D.A., Hoglund, J., 2005. Testing the hypothesis of recent population expansions in nematode parasites of human-associated hosts. Heredity 94, 426–434.
Nadler, S.A., 1995. Microevolution and the genetic structure of parasite populations. J. Parasitol. 81, 395–403.
O'Connor, L.J., Walkden-Brown, S.W., Kahn, L.P., 2006. Ecology of the free-living stages of major trichostrongylid parasites of sheep. Vet. Parasitol. 142, 1–15.
Palcy, C., Silvestre, A., Sauve, C., Cortet, J., Cabaret, J., 2010. Benzimidazole resistance in *Trichostrongylus axei* in sheep: long-term monitoring of affected sheep and genotypic evaluation of the parasite. Vet. J. 183, 68–74.
Posada, D., Crandall, K.A., 1998. MODEL TEST: testing the model of DNA substitution. Bioinformatics 14, 817–818.
Poulin, R., Keeney, D.B., 2008. Host specificity under molecular and experimental scrutiny. Trends Parasitol. 24, 24–28.
Prichard, R., 1994. Anthelmintic Resistance. Vet. Parasitol. 54, 259–268.
Redman, E., PAckard, E., Grillo, V., Smith, J., Jackson, F., Gilleard, J.S., 2008. Microsatellites analysis reveals marked genetic differentiation between *Haemonchus contortus* laboratory isolates and provides a rapid system of genetic fingerprinting. Int. J. Parasitol. 38, 111–122.
Rogers, A.R., 1995. Genetic evidence for a pleistocene population explosion. Evolution 49, 608–615.
Rogers, A.R., Harpending, H., 1992. Population growth makes waves in the distribution of pairwise genetic differences. Mol. Biol. Evol. 9, 552–569.
Rogers, A.R., Fraley, A.E., Bamshad, M.J., Watkins, W.S., Jorde, L.B., 1996. Mitochondrial mismatch analysis is insensitive to the mutational process. Mol. Biol. Evol. 13, 895–902.
Schneider, S., Excoffier, L., 1999. Estimation of demographic parameters from the distribution of pairwise differences when the mutation rates vary among sites: application to human mitochondrial DNA. Genetics 152, 1079–1089.
Sehgal, R.N.M., Jones, H.I., Smith, T.B., 2001. Host specificity and incidence of *Trypanosoma* in some African rainforest birds: a molecular approach. Mol. Ecol. 10, 2319–2327.
Severinghaus, J.P., Brook, E.J., 1999. Abrupt climate change at the end of the last glacial period inferred from trapped air in polar ice. Science 286, 930–934.
Shannon, P., Markiel, A., Ozier, O., Baliga, N.S., Wang, J.T., Ramage, D., Amin, N., Schwikowski, B., Ideker, T., 2003. Cytoscape: a software environment for integrated models of biomolecular interaction networks. Genome Res. 13, 2498–2504.
Singer, F.J., Norland, J.E., 1994. Niche relationships within a guild of ungulate species in Yellowstone-National-Park, Wyoming, following release from Artificial Controls. Can. J. Zool. 72, 1383–1394.
Sommer, R.S., Zachos, F.E., Street, M., Joris, O., Skog, A., Benecke, N., 2008. Late Quaternary distribution dynamics and phylogeography of the red deer (*Cervus elaphus*) in Europe. Quat. Sci. Rev. 27, 714–733.
Tajima, F., 1989. Statistical method for testing the neutral mutation hypothesis by DNA polymorphism. Genetics 123, 585–595.
Theron, A., Sire, C., Rognon, A., Prugnolle, F., Durand, P., 2004. Molecular ecology of Schistosoma mansoni transmission inferred from the genetic composition of larval and adult infrapopulations within intermediate and definitive hosts. Parasitology 129, 571–585.
Webster, L.M.I., Johnson, P.C.D., Adam, A., Mable, B.K., Keller, L.F., 2007. Macrogeographic population structure in a parasitic nematode with avian hosts. Vet. Parasitol. 144, 93–103.
Wilson, D.J., Falush, D., McVean, G., 2005. Germs, genomes and genealogies. Trends Ecol. Evol. 20.
Wimmer, B., Craig, B.H., Pilkington, J.G., Pemberton, J.M., 2004. Non-invasive assessment of parasitic nematode species diversity in wild Soay sheep using molecular markers. Int. J. Parasitol. 34, 625–631.
Wright, S.W., 1931. Evolution in Mendelian populations. Genetics 16, 97–159.
Young, R.R., Anderson, N., 1981. The ecology of the free-living stages of *Ostertagia ostertagi* in a winter rainfall region. Aust. J. Ag. Res. 32, 371–388.